3D Printing a Safer Future:
Alternative Resins for Stereolithography

Rachel Scholes, Lauren Irie, Jacob Manheim,
Kyle Peerless and Ladan Khandel

Greener Solutions, Fall 2019
University of California, Berkeley
December 20th, 2019

BERKELEY CENTER FOR GREEN CHEMISTRY

Table of Contents

Acknowledgements 3

Introduction 4

Approach to Evaluating Alternatives 6

Strategy Overview & Inspiration 9

Strategy 1: Methacrylate-Functionalized Biopolymers 10

Strategy 2: Photoinitiated Click Chemistry 16

Strategy 3: pH-Induced Photopolymerization 19

Strategy 4: Photo-Induced Cross-Linking of Unmodified Proteins 22

Strategy 5: Encapsulation for Release of Reactive Monomers 25

Comparison of Alternatives 28

Conclusions & Recommendations 32

References 35

Acknowledgements

We would like to extend our gratitude to our instructors Meg Schwarzman, Tom McKeag, and Billy Hart-Cooper, as well as our classmates for all of their insights, guidance, and feedback.

We would also like to thank Nicole Panditi for sharing her 3D printing expertise and Justin Bours for offering guidance on the assessment of alternative SLA resins. Finally, we would like to thank Professor Alshakim Nelson and Patrick Smith at the University of Washington for contributing insights into ongoing SLA printing research using alternative chemistries.

Introduction

Stereolithography (SLA) is a type of additive manufacturing that uses ultraviolet (UV) photopolymerization to produce intricate 3D prints from a vat of liquid resin. Estimated at $700 million in 2018, the SLA industry is projected to grow to nearly $9 billion in the next few years due to technological advancements and expanding applications (Kaza *et al*., 2018). SLA produces highly precise and customizable prints used in biomedical applications including implantable devices, tissue engineering, and cell-containing hydrogels (Melchels *et al*., 2010). Already, one of the largest hearing aid manufacturers in the world uses SLA to print 98% of its hearing aids (Sharma, 2013). The same characteristics that advance SLA in the biomedical world also make it useful in other settings. For instance, SLA can rapidly manufacture high-performance prototypes, models, and parts in the aerospace and automotive industries (Schmidleithner & Kalaskar, 2018).

SLA photopolymerizes liquid monomers and oligomers into polymer networks in a layer-by-layer fashion (Varotsis, 2019). First, a computer program slices a 3D digital model into thin layers. Next, UV lasers trace the outline of each layer at the top of a vat of liquid, causing the resin to cross-link and polymerize. Objects are printed from the bottom up as the build platform moves downward in increments that are the height of each cross-sectional layer (Varotsis, 2019).

Current SLA printers use PR48 resin, which consists of the following components by weight percent (Autodesk, n.d.):

Oligomers: Allnex Ebecryl 8210 **39.776%**, Sartomer SR 494 **39.776%**
Monomer: Rahn Genomer 1122 **19.888%**
Photoinitiator: Esstech TPO+ **0.400%**
UV blocker: Mayzo OB+ **0.160 %**

Reactive monomers and oligomers are types of (meth)acrylates used for cross-linking and comprise over 99% of the PR48 resin. Acrylates undergo rapid cross-linking in the SLA context via radical photoinitiation and provide tunable mechanical properties with shrinkage of printed objects (Beach & Kundu, 2010). However, the inherent reactivity of acrylates poses problems to human health and the environment. Health hazards are exacerbated by the 20% to 30% of monomers and oligomers that remain unreacted in the final print and are bioavailable via dermal or inhalation pathways (Beach & Kundu, 2010). Solvent baths remove unpolymerized acrylates, producing hazardous waste.

The reactive monomer and oligomers in PR48 exhibit toxicity across a number of endpoints, particularly genotoxicity, sensitization, skin, eye, and respiratory irritation, and toxicity to aquatic life. Allnex Ebecryl 8210 is an eye irritant, toxic to the aquatic environment, and has a high potential for bioaccumulation (Allnex, 2019). Likewise, Sartomer SR 494 causes serious eye irritation and is toxic to aquatic environments but has less potential for bioaccumulation and is considered inherently biodegradable (Arkema, 2014). Finally, Rahn Genomer 1122 causes severe allergic reactions in mice when exposed at very low levels and induces chromosomal

aberrations *in vitro* (Rahn, 2018). Additional concerns with Rahn Genomer 1122 include skin and eye irritation, toxicity to the respiratory system, toxicity to aquatic life, and low potential for biodegradability (Rahn, 2018). Notably, the reactive monomer and oligomers discussed here lack data on carcinogenicity and reproductive and developmental toxicity.

The minor components of the PR48 resin, including the photoinitiator and UV blocker, also present serious health and environmental hazards. The photoinitiator may cause reproductive toxicity, skin sensitization, and aquatic toxicity (Cheng *et al.*, 2015). The UV blocker may cause skin and eye irritation and is persistent in the environment (Cheng *et al*., 2015).

Given the projected growth of the SLA industry and the significant hazards inherent in the standard SLA resin, greener solutions are necessary to safeguard human health and the environment. We propose five strategies to mitigate the hazards of PR48, focusing on reducing or replacing (meth)acrylate cross-linkers.

Approach to Evaluating Alternatives

In assessing the technical performance of our alternative formulations to PR48, our first priority was to gauge whether our proposed solutions exhibited properties that would enable printability within the SLA context. Through discussions with Nicole Panditi, a researcher in the Berkeley Center for Green Chemistry with expertise in 3D printing, we defined a set of technical performance benchmarks based on properties of SLA resins currently on the market (Table 1). We used these benchmark values to inform our evaluation of the solutions we proposed.

Each of the benchmarks relates to specific aspects of the printing process or reflects properties of the final print. One important criterion is the conversion of monomers and oligomers to cross-linked polymers, which occurs in current printers at a rate of 70-80%. Conversion affects material properties of the final print as well as user exposure to unreacted ingredients. Another crucial characteristic is the curing speed upon light exposure. With existing resins, each layer of an object prints in approximately ten seconds, allowing for quick prototyping of intricate objects. The resin viscosity also affects print speed by determining how quickly liquid resin flows around the moving build platform to form new layers. Both viscosity and curing speed affect layer thickness, which in turn influences the dimensional accuracy of printed parts. Dimensional accuracy measures how closely the dimensions of a printed part match the design in the CAD file. Existing printers are able to create objects with dimensions within 0.10 mm of the expected value. Strength and structural integrity, measured with compressive or tensile strength tests, contribute to durable, long-lasting parts. Existing resins produce parts with strength metrics in the MPa range. Finally, SLA resins allow for the penetration of UV light in order to facilitate photopolymerization and cost approximately $150 per liter.

Table 1. Technical performance of current SLA resins.

Polymerization and Aesthetic	● 70-80% conversion or better ● Smooth surface of printed product
Speed	● Material layer must cure in < 10 sec
Viscosity	● <0.5 Pa*s
Dimensional Accuracy	● +/- 0.10 mm
Layer Thickness	● 50-100um or smaller
Strength	● 1-10 MPa
Clarity	● Resin allows for light penetration
Cost and Commercial Availability	● $150/L or better

Throughout our investigation of alternative formulations, we encountered significant technical data gaps for the metrics described above. For some strategies, our technical performance

evaluation was limited to proof-of-concept demonstrations of novel processes or materials. Confronted with these challenges, we developed a framework to evaluate the most critical technical performance criteria using available data.

Because SLA is primarily used in settings where precision and speed are critical (e.g., hobbyist, research, and biomedical applications), we decided to prioritize evaluating cure time and dimensional accuracy. We also evaluated strength to ensure durability of printed objects, but we allowed for some flexibility in this requirement as SLA is not typically used for objects with high-strength mechanical functions. These criteria are outlined in Table 2, which defines our core targets for speed, viscosity, accuracy, and strength.

Table 2. Technical performance criteria for alternative formulations.

Goal	Target
Speed	Material layer must cure in under 10 seconds
Viscosity	< 500 cps
Dimensional Accuracy	(+/-) 0.10mm
Strength	Tensile Strength, Compressive Strength or Modulus at MPa order of magnitude

We also developed performance criteria for health, environment, and sustainability endpoints, to prioritize solutions with significantly reduced hazards compared to PR48 (Table 3). In particular, we were concerned by the percent unreacted reactive ingredients in the final print, irritation to skin and eyes, sensitization, and aquatic toxicity of the PR48 formula. Wherever possible, we developed specific target values, with which we evaluated our alternative solutions. These targets were based on categories from the Globally Harmonized System, GHS, (e.g. oral toxicity, inhalation toxicity, and toxicity to aquatic life) (United Nations, 2011) or other sources (e.g. biodegradability, bioaccumulation) (ChemSafetyPro, 2019; UK Marine SACs, n.d.). For the percent of reactive ingredients in the final product, hazardous waste generation, and sustainably sourced chemicals, we defined targets that improve upon existing formulas and incorporate industry knowledge provided by our partners.

We applied a standardized approach to evaluate the hazard endpoints in Table 3 for each proposed strategy. First, we consulted authoritative lists, including those published by the International Agency for Research on Cancer (IARC), the National Toxicology Program (NTP), California's Proposition 65 via the Office of Environmental Health Hazard Assessment (OEHHA), and the European Union Registration, Evaluation, Authorisation, and Restriction of Chemicals (REACH) via the European Chemicals Agency (ECHA). In general, these authoritative bodies provided information on well-studied chemicals but failed to examine many of the chemicals in our proposed alternative solutions. Second, we conducted literature reviews and compiled peer-reviewed toxicity data. This step included searching the National Institutes of

Health ToxNet database, which summarizes toxicology findings from peer-reviewed studies. For further toxicity data, we turned to safety data sheets (SDSs) published by chemical manufacturers, such as Sigma-Aldrich. In most cases, these SDSs provided data on GHS classifications for a number of health and environmental endpoints as well as values for lethal doses (LD50s) and the octanol-water partition coefficient, a predictor of bioaccumulation potential. Finally, we attempted to use predictive toxicology software, specifically the EPA's CompTox Chemical Dashboard, to fill in our remaining data gaps. This effort was largely unsuccessful because predictive toxicology provides estimates primarily for small molecules that are structurally similar to other well-studied chemicals. In contrast, the chemicals we examined were often large, polymeric molecules with reactive functional groups. The dearth of toxicity data on these large molecules led us to assess health and environmental endpoints with respect to the raw ingredients used to formulate our proposed resins and to consider the implications of attaching reactive functional groups to large molecules.

Table 3. Health and environmental performance criteria.

	Goal	Target
Human Health	**Low Oral Toxicity**	LD50 > 5000 mg/kg
	Low Inhalation Toxicity	LD50 > 20 mg/L
	Non-irritating to Skin and Eyes	Negative results from in vitro irritation tests or animal tests
	Low Sensitization Potential	Negative results from animal tests
	Minimal Mutagenic and Carcinogenic Toxicity	Negative for chromosomal aberrations, Negative results from Ames test
	Minimal Reproductive or Developmental toxicity	No endocrine disruptors, Negative results from reproductive / developmental toxicity screening assay
	Minimal Unreacted Reactive Ingredients in Final Product	Less than 10%
Healthy Ecosystems	**Biodegradable**	Half life shorter than 40 days in freshwater
	Low Potential for Bioaccumulation	log Kow < 3
	Minimal Toxicity to Aquatic Life	96 hr LC50 > 100 mg/L
	Minimal Hazardous Waste Generated	No generation of hazardous waste
Sustainability	**Chemicals Sustainably Sourced and Manufactured**	Chemicals not derived from fossil fuels

Strategy Overview & Inspiration

We have identified five strategies to reduce or replace (meth)acrylates in SLA printing resins, represented in Figure 1, below. These strategies represent a range of stages in their technological development, and they highlight tradeoffs among our technical, health, and environmental criteria. For instance, our first strategy uses resin that has been tested in an SLA printing context and meets our technical criteria, but hazardous methacrylates pose a risk during resin formulation. Conversely, Strategy 5 proposes the use of encapsulation techniques that are far from being developed for the SLA printing context, and data gaps remain for many of our criteria. We present this range of options as a roadmap for industry leaders to consider investments in what we believe may be transformative innovations in SLA technology.

Biopolymers and processes found in nature inspired our proposed strategies. Using biopolymers in SLA printing opens up possibilities for harvesting raw materials from natural sources, thus replacing petroleum-derived resins with renewable feedstocks. In many cases, the proposed materials are byproducts or waste materials of existing industries, making the raw materials inexpensive and sustainable. Further, we believe that biopolymers may be more likely to exhibit low human toxicity and ecotoxicity, and to be more biodegradable than petroleum-derived polymers.

For each strategy, we propose a photopolymerization process and give example materials for use in resin formulas. We also consider additional steps that could be taken to enhance the properties of objects printed with our proposed strategies - for instance, using post-print curing or additives to enhance strength. Finally, we provide an overview of how each strategy addresses our health and environmental criteria while promising adequate technical performance, and we propose steps that industry leaders could take to further develop these proposed strategies.

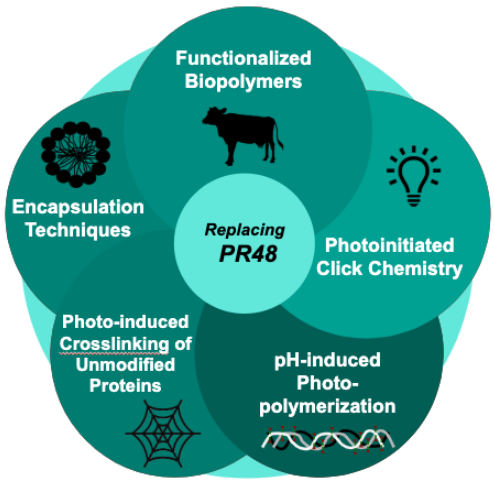

Figure 1. Overview of proposed strategies.

Strategy 1: Methacrylate-Functionalized Biopolymers

In this strategy, we propose to create SLA-printed objects from natural, renewably-sourced biopolymers that are functionalized to undergo photopolymerization. Biopolymers extracted from waste products of the seafood and beef industries attach to acrylate functional groups for polymerization, and additives are used to improve material properties. We were inspired by nature's design of chitin-based materials with proteins as additives to yield materials ranging from the soft bodies of caterpillars to firm shells of shrimp.

Several biopolymers will react similarly when functionalized using analogues approaches. Here we provide two detailed examples, based on functionalized forms of commercially available biopolymers: bovine serum albumin (BSA) and chitosan. The beef industry produces BSA, a protein found in the blood of cows (Meat and Livestock Australia, 2001). The seafood industry produces waste chitin, which is extracted and deacetylated to produce chitosan. Both materials photopolymerize when functionalized with acrylate groups, making them ideal for use with this strategy.

Technical Performance

Our primary example of this strategy uses methacrylate-functionalized BSA, which has recently been demonstrated for use in SLA printing (Smith *et al.*, 2019). During resin formulation, lysine functional groups on BSA react with methacrylic anhydride. The reaction transforms lysine groups to methacrylamide groups and can be achieved with >90% conversion. The functionalized BSA is then purified to remove residual methacrylate anhydride or other small molecules. The resin includes BSA dissolved in water along with a photoinitiator system: ruthenium tris(bipyridyl) chloride ($Ru(bpy)_3Cl$) and sodium persulfate (SPS). Alternative photoinitiators may also be used (from personal communication with Professor Alshakim Nelson and Patrick Smith, University of Washington), and may be desirable because of the cost and hazards associated with ruthenium catalysts. The ruthenium-based photoinitiator is discussed here due to its previous use and compatibility with the 405-nm light source of existing commercial SLA printers.

Additional reactive acrylate oligomers — poly(ethylene glycol) diacrylate (PEG-DA, Mn 700 Da) or poly(ethylene glycol) methyl ether acrylate (PEG-A, Mn 480 Da) — were added during demonstration of this resin to improve the printability, cure time, and mechanical properties of the resulting print. This formulation has been used to print both hydrogels and bioplastic constructs using a standard SLA printer: the Formlabs Form 2 printer. Images of printed BSA-based lattices and scanning electron microscopy (SEM) images of the prints showing their fine layer thickness are found in Figures 2 and 3.

Further research on methacrylate-functionalized BSA has iterated on the resin formulation and post-print processing steps to optimize technical performance. Resins with low viscosity (less than 3.4 Pa·s), and a fast cure rate were achieved. The as-printed BSA structures were

hydrogels with water content that reached 60% by weight. To make these hydrogels into rigid structures with better mechanical properties, the printed objects were subjected to a post-print curing step under 400-nm light for 1.5 hours for further cross-linking. After the post-print curing step, the prints were dehydrated and thermally cured at 120°C for 180 min. This step was denatured the BSA protein, increasing hydrophobic and hydrogen bonding interactions, and turning the product into a bioplastic rather than a hydrogel. The finding that post-print processing drastically enhanced the strength of SLA-printed objects excites us because these post-print steps create object that achieve our technical performance criteria. Further, post-print processing could potentially be applied to other SLA-printed hydrogels to improve mechanical properties. Additionally, in the case of BSA, objects can be rehydrated to the hydrogel form (Smith *et al.*, 2019). With this technology, a single SLA formulation could be used for a variety of applications, including biomedical hydrogel applications as well as applications with stricter mechanical property requirements.

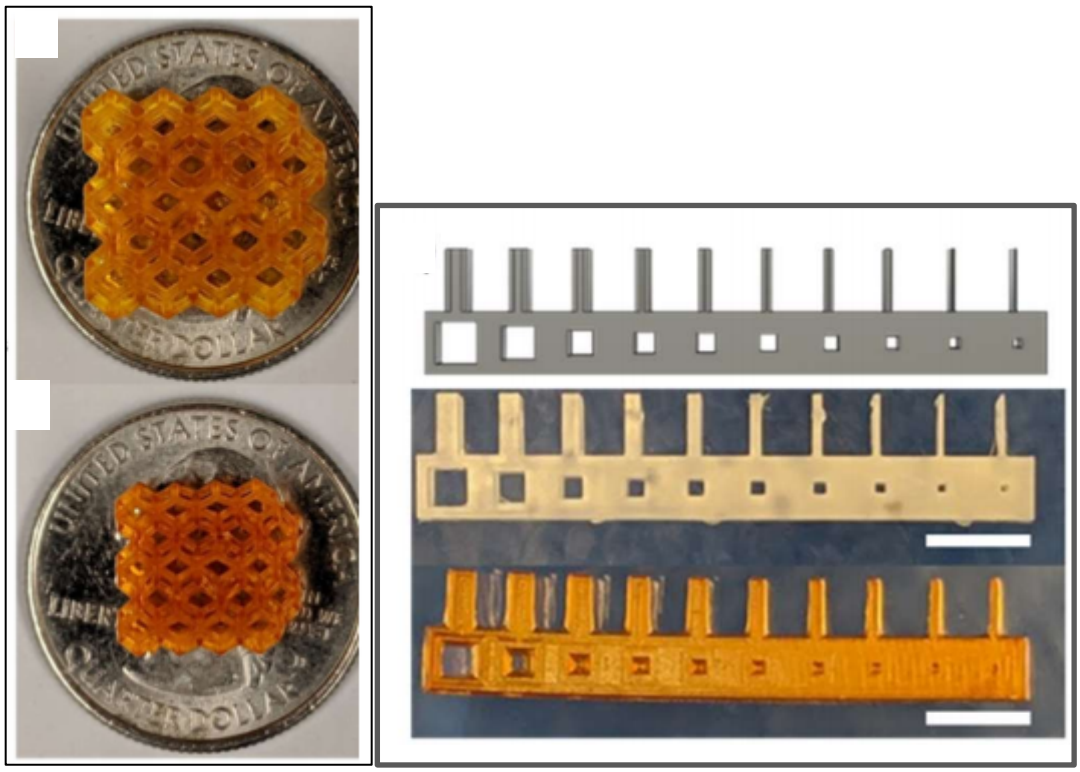

Figures 2 and 3. Scale of as-printed swollen hydrogel vs. cured prints and dimensional accuracy testing of BSA prints (Smith *et al.*, 2019).

The cured BSA-based plastics met or exceeded all of our core technical performance criteria (Table 4), indicating that these materials are a well-developed technology that could be implemented in existing SLA printers with little further development. In addition to our core metrics, the BSA biopolymer demonstrated a modulus in compression testing of roughly 6 MPa (roughly 870 pound-force per square inch), meaning the prints do not deform until exposure to stresses at this level, comparable to moduli of prints using current SLA resins.

Table 4. Key performance properties of BSA-based biopolymers relative to technical performance criteria (Smith *et al.*, 2019).

Metric	**Industry Standard**	**BSA-MA Methods**
Viscosity	< 0.5 Pa*s	0.267 Pa*s
Curing Speed	<10 seconds	2.2 seconds
Dimensional Accuracy	+/- 0.1 mm	+/-0.07 mm

Biopolymers besides BSA may also be modified with methacrylic moieties or blended with a methacrylated biopolymer and are a promising avenue for further investigation. Chitosan, for example, has been modified with acrylate groups and used for tissue engineering and drug delivery applications. Chitosan-based resins are limited by the low solubility of chitosan in neutral or high pH solutions, but chitosan can by solubilized by attaching lactic acid and methacrylic acid functional groups (Hu *et al.*, 2008).

Modified chitosan method has previously been used in precise bio-tissue or drug delivery settings and is expected to exhibit limited human health effects based on its use in a range of biomedical applications (Sikia *et al.*, 2015). Chitosan-based products can be synthesized at small scales with great precision. However, data gaps remain for core technical performance criteria including dimensional accuracy, speed, and long-term integrity of printed objects. Chitosan-based hydrogels have been cross-linked in molds within 4 minutes, but this information is difficult to compare to our criteria for layer-by-layer curing in under 10 seconds (Hu *et al.*, 2008). Chitosan-based hydrogels also undergo significant weight loss due to water loss, which indicates a lack of long-term structural integrity. From a strength point of view, chitosan-based materials do not currently meet our criteria, with reported storage modulus values between 0.8-7 kPa, which is roughly 1,000 times lower than our benchmark (Hu *et al.*, 2008).

The poor mechanical properties of chitosan-based materials can be improved using additives, similar to the hardening of natural chitin-based materials by addition of protein (in shrimp shells and fish scales, for instance). Research in dental and bone engineering produces chitosan-based scaffolds with varying mechanical properties, water retention, cytotoxicity, and degradation. Some examples of commonly used chitosan additives are bioactive glass, which increases strength and has been blended with additional materials like carbon nanotubes and polylactic-co-glycolic acid (PLGA) nanoparticles. For example, bioactive glass-chitosan scaffolds can increase compressive strength relative to chitosan alone from 34 to 363 kPa, and ca increase the compressive modulus from 0.41 to 10.04 MPa (Pourhaghgouy *et al.*, 2016). More examples can be found in Table 5.

Table 5. Chitosan-based scaffolds for increased mechanical properties (Jarosz *et al.*, 2019).

Polymer / Molecule Additive	**Observations as Compared to the Properties of Chitosan Polymer Scaffolds Alone**	**Metric**
Bioactive Glass	Decreased water retention, increased biodegradation and mechanical properties	Compressive Strength: 34 to 363 kPa Compressive Modulus: 0.41 to 10.04 Mpa
Gelatin and β-tricalcium phosphate	No cytotoxicity at low concentration, decreased biodegradation, and increased mechanical properties	Young's modulus: 0.02 MPa to 0.4 MPa Compressive Strength: 0.2 to 0.52 MPa
Gelatin and hydroxyapatite	No cytotoxicity, increased osteogenesis and mechanical properties	Compressive strength: 3.5 MPa
Poly(vinyl alcohol) Collagen Bioglass	No cytotoxicity, increased biomineralization and mechanical properties, decreased water retention and biodegradation	Compressive Modulus: 214.64 MPa Compressive strength: 11.49 MPa

In conclusion, BSA and chitosan are promising materials for SLA printing. Extensive research has demonstrated these two biopolymers for use in hydrogels, and recent work indicates that mechanical properties can be enhanced via post-print curing steps. Chitosan's mechanical properties can also be improved through the addition of bioactive glass, collagen, and other additives. We recommend further optimization of technical performance criteria such as viscosity, cure rate, resolution, and strength for these promising materials.

Health and Environmental Performance

Our functionalized biopolymer strategy employs several ingredients, each with a unique hazard profile. Formula components include a photoinitiator and functionalized biopolymer. Although this report focuses on BSA functionalized with methacrylic acid, there are other cross-linking options that may offer differing health and environmental performances across endpoints of interest (as well as varying mechanical properties). Table 6, below, includes components of BSA- and chitosan-based alternatives along with a brief summary of the available hazard data in order to provide guidance for future inquiry, while the remainder of this section delves into the health and environmental performance of BSA-based resins.

For BSA-based resins, the formulation process is likely to pose greater risks than resin use during printing. During resin formulation, BSA is functionalized with methacrylic acid, which is a reactive component that presents health hazards. Conversely, this reactive component is not present, at least to any comparable degree, during the printing process. This shift reduces the risks posed by our strategy relative to the current PR48 formula, which requires SLA users to

directly interact with a reactive monomer and oligomers. Functionalizing BSA with methacrylate groups results in polymer building blocks that have high molecular weights and are therefore less bioavailable than the methacrylates by themselves. Hence, in this strategy, the health risks associated with the methacrylates are mostly limited to the occupational setting during resin formulation.

BSA is essentially nontoxic and while functionalizing BSA with methacrylate groups may increase toxicity, the high molecular weight of the polymers reduces its bioavailability, as described earlier. Efforts to predict the toxicity of BSA functionalized with methacrylic acid using computational toxicology tools proved unsuccessful, likely because computational toxicology programs are not well-suited for assessing polymers. Consequently, there remain significant data gaps due to the difficulty of obtaining reliable information from predictive software and the lack of direct toxicological data regarding functionalized BSA. However, polymers themselves are rarely toxic. The three BSA-based resins that have successfully been printed contained additional acrylate components (weight percent was 5-10% PEG-DA or PEG-A). Despite the hazards associated with adding these acrylate cross-linkers, the lower weight percent and the higher molecular weight of these cross-linkers relative to the components of PR48 imply lower exposure and lower bioavailability. Furthermore, these cross-linkers were included to improve the technical performance of the print, which could potentially be sacrificed to some extent in order to reduce the use of acrylate comonomer.

While the primary aim of this report is to tackle issues related to the reactive monomer and oligomers of the PR48 formula, an alternative photoinitiator, Irgacure2959, was identified for this strategy based on its use with photo-cured chitosan-based resins (Hu *et al.*, 2008). The existing photoinitiator in the PR48 formula is a reproductive toxicant, skin sensitizer, and aquatic toxicant. In contrast, a study conducted at Johns Hopkins University found that Irgacure2959 “is well tolerated by many cell types over a range of mammalian species” (Williams *et al.*, 2005). The promising health characteristics of Irgacure2959 warrant further investigation.

Table 6. Summary of health and environmental impacts and data gaps.

Chemical Name	Function in Final Product	Identified Health and Environmental Impacts	Data Gaps	Data Sources
BSA-MA-LA	Functionalized polymer	- Virtually non-toxic when ingested - Not expected to bioaccumulate	- No animal or human toxicity studies	EPA CompTox (Nearest Neighbor results)
Irgacure2959	Photoinitiator	- Well tolerated by many cell types over a range of mammalian species	- No animal or human toxicity studies	*Biomaterials*, 2005
Lactic Acid	Intermediate in functionalization	- Very high hazard for: skin corrosion / irritation (GHS Category 1 / H314) And serious eye damage / eye irritation (GHS Category 1 / H318) -Moderate hazard: Acute oral toxicity (GHS 6.1D)	- Potential concern: Very toxic to aquatic life (GHS H400) - May be corrosive to metals (GHS H290)	Pharos Hazard Assessment
Methacrylic Acid	Intermediate in functionalization	- Very high hazard for: severe skin burns and eye damage (GHS H314) - Specific target organs/systemic toxicity following single exposure (GHS Category 1 / H370) - Hazardous to the aquatic environment (acute) (GHS Category 3 / H402)	- Potential neurotoxicant	Pharos Hazard Assessment
BSA (bovine serum albumin)	Alternative biopolymer to functionalize with acrylates	- Moderate to high hazard for Asthmagen (Rs) - sensitizer-induced by the Association of Occupational and Environmental Clinics (AOEC) - However, this hazard is minimized as the product will be dissolved in an aqueous solution	- None observed	SDS Pharos Hazard Assessment
Chitosan	Alternative biopolymer to functionalize with acrylates	- No observed toxicity in male rats given 5,200 mg chitosan/kg body weight per day or in female rats given 6,000 mg/kg per day	- None observed	NTP Technical Report on the Toxicity Study of Chitosan

Strategy 2: Photoinitiated Click Chemistry

Building on Strategy 1, we investigated the possibility of functionalizing biopolymers with other reactive functional groups that undergo cross-linking reactions. In particular, we considered “click” chemistry reactions - those that react selectively, at high yield. The inspiration for click chemistry builds on nature’s use of small, modular units to build polymers through common linkage types. For instance, the formation of proteins from amino acids relies on selective addition of monomer units to a growing chain. Biology accomplishes this goal using enzymes that facilitate specific, high-yield reactions. In recent years, chemists have discovered several reaction types that are also specific without the need for an enzyme or catalyst, and in some cases, these reactions can be photoinitiated.

Here we suggest the modification of biopolymers with functional groups that undergo photo-induced click chemistry reactions. In particular, we suggest the use of Diels-Alder reactions with functionalized lignin. Lignin is a desirable feedstock because it is a waste product of the biomass and ethanol industries with few existing applications. Diels-Alder reactions can occur without a photoinitiator, removing a resin component that contributes substantially to toxicity. Diels-Alder reactions have been demonstrated in the context of photoinduced polymerization with polyethylene glycol (PEG) and can also yield stable polyimides (Meador *et al.*, 1996) and acrylic ester copolymer blends (Tyson *et al.*, 2005).

Technical Performance

This strategy has been demonstrated most comprehensively with a functionalized PEG backbone. PEG was functionalized with maleic acid and benzophenone, then irradiated with a 320-nm lamp. Upon irradiation, the maleic acid and benzophenone functional groups underwent cross-linking reactions, leading to the formation of solid structures without the addition of a photoinitiator (Winkler *et al.*, 2012).

We propose to implement this strategy with a functionalized lignin backbone. Lignin is amenable to functionalization because it contains hydroxyl groups. Lignin can be functionalized with maleimide and undergo a Diels-Alder reaction to form lignin polymers at high yield (Buono *et al.*, 2017). In the demonstration of this technique, maleimide-functionalized lignin was cross-linked at elevated temperature with furan-containing cross-linker molecules. The furan functional group reacts with maleimide similarly to the reaction between maleic acid and benzophenone, though in this case the reaction was not photoinitiated. Though this technique has only been demonstrated with a separate furan-based cross-linker, we propose to decrease resin toxicity by attaching a furan or benzophenone functional group to the lignin backbone. In this configuration, the Diels-Alder reaction can occur between two functional groups attached to biopolymers, without an external photoinitiator, such that all the resin ingredients have a high molecular weight and low bioavailability.

For the case with maleimide-functionalized lignin, objects were printed over the course of several hours, and not in a layer-by-layer method (Buono *et al.*, 2017). Without information about the amount of material printed, we were unable to accurately assess the rate of curing, but we note that the demonstrated speed (on the scale of hours) is much too slow relative to our technical criteria. We recommend further testing of this approach in a layer-by-layer printing context to assess and improve on the rate of polymerization.

We used the results of tensile tests conducted on printed "dogbone" samples (Figure 4) to assess the strength of objects printed with this strategy. The tensile strength increased with greater linker functionality, meaning cross-linkers with four furan groups provided enhanced strength relative to cross-linkers with two furan groups. Overall, the strength of these lignin-based materials approached 4 MPa, which is meets our technical performance criterion.

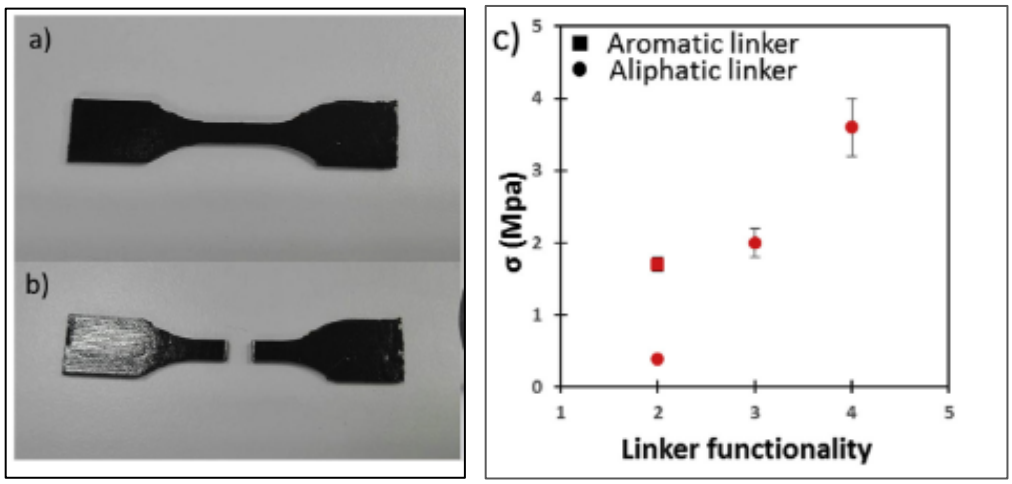

Figure 4. Tensile test samples and yield strength results using lignin-based strategy (Buono et al., 2017).

This strategy could potentially also be implemented with other biopolymers or alternative click chemistry reactions. For example, chitosan functionalized with furan and maleimide groups has been demonstrated to form cross-linked hydrogels (Guaresti *et al.*, 2017). Other click chemistry reactions could also be utilized for cross-linking, but have not been demonstrated in a photopolymerization process. Thiol-ene reactions have been proposed for polymerization, and can be photoinitiated, but are sensitive to oxygen and require further development (Radl *et al.*, 2017; Kim *et al.*, 2019). Photoinitiated click chemistry has recently gained interest in biomedical applications (Herner and Lin, 2016), and we believe research in this area may yield technologies relevant to SLA printing and should be kept in mind for future innovations.

Health and Environmental Performance

Similar to the first strategy, the health risks associated with photo-initiated click chemistry are generally low to users during the printing stage but remain a concern for workers who are involved in the functionalization of lignin with benzophenone or furan and maleic acid. Benzophenone, in particular, exhibits troubling features across a number of important

endpoints. The chemical is a possible human carcinogen (IARC Group 2B), a suspected endocrine disruptor, and is classified under the most hazardous GHS categories for both acute and chronic aquatic toxicity (IARC, 2012; ToxNet, 2015a). Across most of these endpoints, maleic acid is less hazardous. When tested on Salmonella strains, maleic acid and its metabolites were found to be not mutagenic (ToxNet, 2015b). Likewise, maleic acid did not exhibit estrogenic properties in female rats and is readily biodegradable (ToxNet, 2015b). However, human toxicity data indicate that maleic acid is seriously irritating to the eyes and mildly irritating to the skin as a 20% aqueous solution (ToxNet, 2015b).

The risks associated with each of these hazards is greatly reduced after benzophenone and maleic acid are attached to lignin, an abundant component of plant cell walls that is virtually non-toxic. Lignin is a large molecule and is therefore less prone to penetrate skin or volatilize. Moreover, lignin's widespread availability from renewable feedstocks meets our target for sustainability. Finally, the lack of a photoinitiator in this strategy presents a major health benefit compared to PR48, which contains a toxic photoinitiator. Overall, this strategy represents an elimination of the hazardous photoinitiator and a significant decrease in the use of reactive small molecules at the printing stage.

Strategy 3: pH-Induced Photopolymerization

Changes in pH commonly induce phase changes, a property that is utilized in this strategy for UV curing. The inspiration for pH-induced phase changes comes from the mussel, which attaches itself to wet surfaces in as little as 30 seconds by secreting acid and byssus-building proteins (Waite, 2017). Upon introduction to the higher-pH seawater environment, proteins cross-link with iron to form a strong anchor for the mussel body (Holten-Andersen *et al.*, 2011). Similarly, localized pH changes can be achieved in SLA printing using a photo base generator (PBG). PBGs absorb light and release bases, which increase the pH and can lead to pH-induced reactions. Previous research conducted by a Greener Solutions team proposed several PBGs for use in SLA printing (Cheng *et al*., 2015). Their report suggested using pH-induced photopolymerization with PBGs to induce inorganic mineral phase precipitation, for instance the formation of calcium carbonate, or photoinitiated cross-linking of protein-mineral phases using a common protein in mussel byssal threads. The combination of organic and inorganic materials introduces the possibility of tuning mechanical properties by varying the component proportions in the resin formula, making this strategy attractive. However, the protein suggested (DOPA, or dihydroxyphenylalanine) is a known developmental toxicant. Further, catechols (e.g., DOPA) as a chemical class are broadly toxic, so the strategy of inducing complexation via this reaction mechanism relies on an inherent hazard (Schweigert *et al.*, 2001).

Here we build on previous work to suggest another possible mineral-organic material which we believe presents a lower hazard profile. We focus on collagen, the most abundant protein in mammals and a major component of bone, skin, muscles, tendons, and ligaments. Collagen has a triple helical structure that makes it very strong among proteins. Collagen is widely available and can be purified from animal sources (Noff and Pitaru, 2003; Wahl and Czernuszka, 2006). Collagen cross-linked with the reducing sugar ribose has been 3D printed in biomedical applications, and its material properties are enhanced by the incorporation of a calcium phosphate mineral phase, hydroxyapatite. We propose SLA printing of collagen-ribose-hydroxyapatite structures via localized pH change induced by a PBG.

Because previous work has considered PBGs in some detail, here we focus on the novel collagen-based materials we propose. Recently, researchers have 3D-printed collagen for biomedical applications via pH-induced gelation using a method known as FRESH (Lee *et al.*, 2019). In this method, acidified collagen solution is brought to pH 7.4 and rapidly forms a collagen filament with 20-um resolution. We propose that a similar technique could be used in SLA, but with PBGs inducing the pH change.

Technical Performance

Inkjet-printed collagen-hydroxyapatite composites create precise structures for bone scaffolding (Figure 5). Able to print cross-sections at the micrometer scale, this method is likely to meet our dimensional accuracy criteria (Lee *et al.*, 2019). As this technology is further developed, one challenge may be maintaining low viscosity. Collagen-containing blends exhibit higher viscosity

than hydroxyapatite alone, which introduces printing challenges in inkjet printers (Inzana *et al.*, 2015) and can decrease dimensional accuracy in SLA printers.

Demonstrations of 3D-printed collagen often lack information regarding strength. We found that the use of collagen alone results in a relatively weak material that is improved upon by taking advantage of organic-inorganic interactions. Flexural strength of 3D-printed collagen-hydroxyapatite composites has been reported to reach 10-80 kPa (Inzana *et al.*, 2015). This range is two orders of magnitude below our benchmark value for tensile strength, but also uses a different test method, making the values difficult to compare.

Collagen-hydroxyapatite composites prepared by other methods have been used for hard tissue repair and can be formed by changing the pH of a bulk solution (Wahl and Czernuszka, 2006). Several collagen-hydroxyapatite composite materials are now commercially available for bone repair applications, and collagen-hydroxyapatite composites produced for bone scaffolds can reach ultimate tensile strengths of 6-60 MPa (Wahl and Czernuszka, 2006).

A number of approaches could further increase material strength of objects printed using this strategy. For instance, the ratio of collagen to calcium phosphate can be adjusted. Higher collagen concentrations yield higher strength materials relative to calcium phosphate alone. Material strength can be further enhanced via glycation, or the cross-linking of collagen with a reducing sugar such as ribose. Glycation has been found to increase the compressive modulus of collagen-based materials by three times (Mason *et al.*, 2013). Ribose-cross-linked collagen-hydroxyapatite composites improve on the mechanical properties of collagen (Krishnakumar *et al.*, 2017). Ribose can also cross-link collagen with hydroxyapatite, making it an ideal cross-linker (Noff and Pitaru, 2003). pH-induced formation of collagen-ribose-hydroxyapatite materials has been demonstrated to achieve cytocompatible scaffolds for bone tissue regeneration (Krishnakumar *et al.*, 2017).

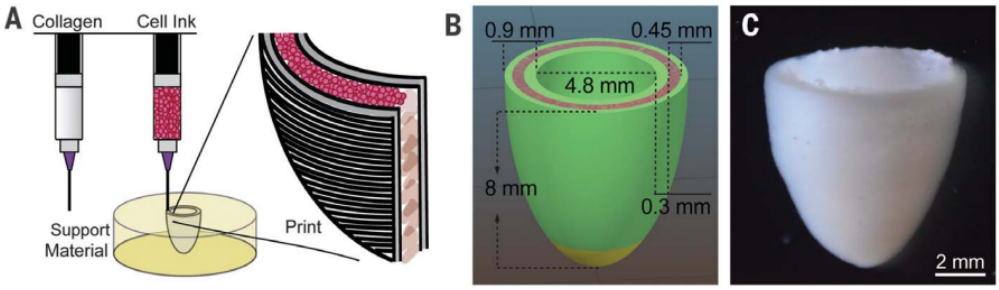

Figure 5. Dimensional drawings and existing collagen printing methods (Inzana *et al.*, 2015).

Health and Environmental Performance

The predominant components of the resin in the pH-induced photo-polymerization strategy are relatively non-hazardous to humans and the environment. Collagen is non-toxic and consumed as a dietary supplement up to 750 mg/day (Norwegian Scientific Committee for Food Safety,

2016). However, collagen may be sourced from fish skin, which could present problems for those allergic to seafood. Hydroxyapatite, used to strengthen the cross-linked material, is an inorganic mineral that is abundant in nature and the human body. It is an important component in bone and tooth material and is considered virtually non-toxic (ToxNet, 2000). Similar to collagen, ribose is abundant in the human body and not expected to present any significant toxicity hazard.

As mentioned above, ribose-mediated cross-linking of collagen-hydroxyapatite requires the use of a photo base generator (PBG), which is the most hazardous component involved in the polymerization process. The 2015 greener solutions team investigated PBGs and found that tertiary ammonium salts were most feasible and posed the lowest health risk because they are soluble in water and release strong bases with high efficiency and yields (Cheng *et al.*, 2015). This allows tertiary ammonium salts to be utilized in relatively low concentrations. The 2015 team examined four of these PBGs in detail, including Ketoprofen, 1,5 diazabicyclo[4,3,0]non-ene (DBN), Phenylgloxylic Acid, and Phenethylamine. Toxicity findings are summarized in Table 7 below. In general, the highest known hazards associated with the tertiary ammonium salt PBGs are skin, eye, and respiratory irritation followed by acute mammalian toxicity and other ecotoxicity.

Table 7. Assessment of PBGs adapted from 2015 Greener Solutions Report.

	Human Health Group I					Human Health Group II								Environmental Health			Environmental Fate	
	Carcinogenicity	Mutagenicity & Genotoxicity	Reproductive Toxicity	Developmental Toxicity	Endocrine Activity	Acute Mammalian Toxicity	Systemic Toxicity & Organ Effects	Neurotoxicity	Skin Sensitization	Respiratory Sensitization	Skin Irritation	Eye Irritation	Respiratory Irritation**	Acute Aquatic Toxicity	Chronic Aquatic Toxicity	Other Ecotoxicity**	Persistence	Bioaccumulation
Ketoprofen	U	U	U	U	U	MH	U	U	U	U	MH	MH	U	U	U	MH	U	U
DBN (1,5-diazabicyclo[4.3.0]non-5-ene)	U	U	U	U	U	U	U	U	U	U	HH	HH	U	U	U	U	U	U
Phenylgloxylic acid	U	U	U	U	U	MH*	U	U	U	U	HH	HH	HH	U	U	U	U	U
Phenethylamine	U	U	U	U	U	MH	U	U	U	U	HH	HH	U	LH	U	MH	U	U

HH: High Hazard	MH: Medium Hazard	LH: Low Hazard	U: Unknown Hazard	* Classification based information not sourced from Pharos or an authoritative body ** Endpoint not included in GreenScreen hazard framework

Strategy 4: Photo-Induced Cross-Linking of Unmodified Proteins

From spider webs to squid beaks, many biological structures found in nature are made up of proteins, which owe their diverse properties and architectures to their fundamental building blocks. Spider silk, for example, is made up of four major protein structures: ß-sheets, Gly II-helices, ß-spirals and random coils. These structures give spider silk tunable mechanical properties that are comparable to synthetic polymers like Kevlar. Beyond stellar mechanical properties, spider silk proteins are also biocompatible, biodegradable, and not cytotoxic (Gil, 2018). These favorable qualities have made spider silk proteins desirable in biomedical applications such as hydrogels and have prompted scientists to synthesize and modify these proteins.

Technical Performance

One way in which proteins have been cross-linked in the laboratory is through an analytical technique called photo-induced cross-linking of unmodified proteins (PICUP) which has been commonly used to observe protein architectures and protein-protein interactions. Recently, this analytical technique has been optimized to fabricate hydrogels of diverse mechanical and physical properties using recombinant spider silk proteins (rSSp) (Gil, 2018). PICUP requires a catalyst called tris(2,2'- bipyridyl) dichlororuthenium(II) hexahydrate (ruthenium), ammonium persulfate (APS) as an electron acceptor, and a high-intensity light source that initiates the reaction. Upon exposure to light, the Ru(II) catalyst is activated and reacts to form a covalent C-C bond between tyrosine moieties on the target protein.

For hydrogel fabrication, recombinant spider silk proteins (rSSp) were produced in the milk of genetically modified goats, purified, washed, and lyophilized. A particular protein, recombinant major ampullate spidroin 1(rMaSp1), was utilized for these hydrogels due to the large proportion of tyrosine groups and the abundance of this protein in spider silk. The spider silk-containing resins were injected into a dog-bone shaped mold and irradiated using a built-for-purpose light source, which induced essentially instantaneous cross-linking.

This method resulted in the highest levels of strength out of any of our strategies. Depending on the post-treatment method (discussed below), the cross-linked hydrogels achieved strengths as high as 13 MPa with modulus values (measure of stiffness) of over 100 MPa (Table 9). These values satisfy our strength criterion and make these materials highly promising.

Further research is needed to fill data gaps regarding other technical performance criteria. This strategy currently has only been demonstrated in cases where resin was injected into molds and subsequently cross-linked. Demonstration of its use in an SLA printer is needed to determine layer-by-layer print speed, although the claim of instantaneous cross-linking in a 1-mm layer indicates that thinner layers used in SLA printing could likely be printed in less than 10 seconds, meeting our speed criterion. The viscosity of the resin was not reported, making it impossible to

assess the potential dimensional accuracy of an SLA-printed object. The built-for-purpose light source used in this demonstration would require modification to be used in an SLA printer, especially with respect to its cooling mechanism, energy-usage, and narrowing the light beam in order to create the precise architectures (Gil, 2018).

Post-modification procedures to tailor material properties present an added value associated with this strategy. After photopolymerization, the resulting hydrogels can be soaked in baths of different solvents (methanol, isopropyl alcohol, and ethanol) to obtain structures with different mechanical and physical properties. A foam-like hydrogel, for instance, can produced by vortexing the resin prior to cross-linking. These different post-modifications and their respective physical properties are outlined in Table 8.

Table 8. The post-cure treatment of the hydrogels and their respective physical properties and images (Adapted from *Gil, 2018*).

Post Treatment	**IPA**	**IPA Frozen**	**Methanol**	**Ethanol**	**Foam** (lyophilization)	**Sponge** (lyophilization + water bath)
Physical Properties	Opaque, white, glass-like, rigid with minor flexibility	White, translucent edges, cartilage like, pulls apart in striations	Solid white, flexible, stretches, compressed has rebound	Solid white, decrease flexibility, stretches less than methanol	White, airy, "packing peanut," soft, floats	Translucent white, porous, retakes form when compressed with addition of water
Result						

Despite data gaps regarding cure speed and the ability to print in an SLA context, we recommend pursuit of this strategy based on the extraordinary strength and tunability demonstrated thus far.

Table 9. Average mechanical results for post-treated cross-linked hydrogels tested in uniaxial tension (Gil, 2018).

Sample	**Max Stress (MPa)**	**Max Strain (mm/mm)**	**Energy to Break (MJ/m^3)**	**Young's Modulus (MPa)**
IPA	13.23 ± 2.42	0.43 ± 0.18	4.27 ± 0.96	101.00 ± 18.66
IPA frozen	9.72 ± 2.13	0.23 ± 0.06	3.77 ± 0.41	78.4± 10.08
Methanol	3.09 ± 0.52	0.26 ± 0.08	0.82 ± 0.02	5.22 ± 0.65
Ethanol	2.75 ± 0.38	1.51 ± 0.30	2.61 ± 0.31	4.07 ± 0.48

Health and Environmental Performance

The spider silk strategy employs recombinant spider silk proteins (rSSP) along with ruthenium and ammonium persulfate catalysts in a water-based formula. Dams-Kozlowska *et al.* (2012) found that rSSPs, which are the predominant component of this formula, were not cytotoxic and did not activate macrophage responses except at the highest concentrations tested (1000 µg/ml). Although this study did not conduct toxicity assays across every endpoint of interest, the results are promising.

The catalysts involved in this strategy present some concerning health and environmental issues. Ammonium persulfate is classified in the highest GHS categories for respiratory sensitization and skin sensitization, on par with the acrylates of the PR48 formula. Additionally, manufacturer safety data sheets list skin and eye irritation, specific toxicity to the respiratory system, and acute aquatic toxicity as potential hazards (Sigma Aldrich, 2014). While ammonium persulfate has many of the same issues as the reactive oligomers and monomer of the PR48 formula, its concentration in the spider silk formula is only 5.04 mM, a much smaller concentration than the acrylates that make up over 99% of the PR48 formula (Gil, 2018).

For the ruthenium catalyst, toxicity data was largely unavailable. The only reported value from the chemical manufacturer for Tris(2,2′-bipyridyl)dichlororuthenium(II) hexahydrate includes an LD50 of 1.999 mg/kg for intravenous injection in mice (Sigma Aldrich, 2019). Hence, data gaps plague ruthenium across nearly every health endpoint. Further complicating the use of ruthenium is that it is one of the rarest metals on earth and can only be mined in certain areas of the world (Sahu *et al.*, 2018). Apart from being expensive, alternative solutions that use ruthenium are not particularly sustainable. However, ruthenium comprises only a miniscule portion of the overall formula at 31.35 µM, a concentration that is over 100 times smaller than that of ammonium persulfate. Should this solution be adopted with ruthenium, we recommend integrating recapture techniques that avoid the disposal of ruthenium as waste.

The ruthenium catalyst and ammonium persulfate used in the resin are a common pair of chemicals used as photoinitiators, but could be substituted with an alternative photoinitiator, as discussed in the context of Strategy 1 (functionalized biopolymers). Due to the high cost and large gaps in toxicological data on ruthenium-based catalysts, we recommend prioritizing alternatives to this photoinitiator system.

Strategy 5: Encapsulation for Release of Reactive Monomers

Encapsulating the highly reactive components of SLA resins could reduce the risk to users and the production of hazardous waste. While the reactivity of photoinitiators, oligomers, and monomers makes them ideal for SLA printing, it also makes them toxic. This inherent tradeoff of current SLA resins inspired us to rethink exposures during SLA printing. What if we could control the exposure of the user to a specific chemical? We propose the creation of a “smart” encapsulation technique that can release and re-collect reactive molecules upon exposure to stimuli, such that release of reactive components is photoinitiated and hazardous components can be recaptured to mitigate exposure to hazardous substances.

Technical Performance

Scientific literature describes a plethora of different stimuli-sensitive encapsulation techniques, such as cyclodextrins, MOFs, and micelles. Micelles are materials made up of nonpolar and polar components, which allow them to self-assemble into a capsule-like configuration, in which their polar components face outwards and their non-polar components face inwards (or vice versa if using a non-polar solvent). Polymeric micelles are highly tunable and have been extensively researched for biomedical applications, specifically drug delivery. Important considerations for drug delivery vehicles include the amount of a chemical released, type of chemical, location of release, and speed of release. Each of these parameters can be controlled by tuning micelle properties including polymerization degree, architectures, and functional group modifications. Similar considerations are important during SLA photopolymerization, making micelles a potentially useful tool to control monomer release in SLA printing.

An ideal encapsulation technique would be able to enclose cross-linkers or reactive monomers/oligomers and release them upon exposure to UV light. Upon release, the reactive components will either 1) react with other resin components spontaneously or upon additional UV exposure, or 2) cross-link with themselves upon exposure to UV light similar to existing methacrylate resins (Figure 6). After an object is printed, the unreacted cross-linkers can be re-encapsulated, separating these toxic and volatile components from users of the printed object.

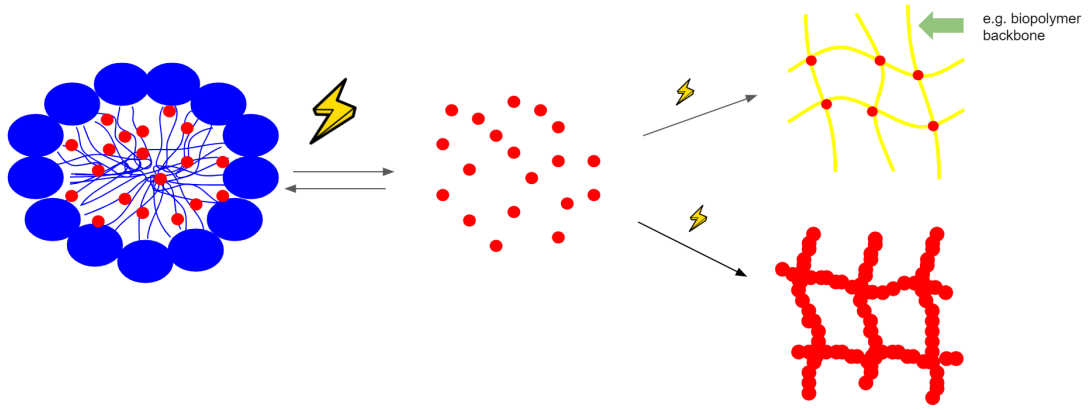

Figure 6. Upon exposure to UV light, a micelle or other encapsulation technique can release cross-linkers which either 1) react with a polymer backbone in the resin or 2) cross-link and polymerize with themselves upon UV irradiation.

A demonstration of the capabilities and properties of micelles is found in a study by *Son et al*. (2014), which describes the synthesis and performance of a spiropyran hyperbranched polyglycerol micelle. Recent advancements in polyglycerol synthesis have led to well-defined, stable architectures with tunable physicochemical properties. The spiropyran is a commonly used functional group for light-responsive micelles due to its unique tunability, stability, and fast response time. When irradiated with UV light, spiropyrans reverse their polarity, collapsing the micelles and releasing their contents. Upon subsequent exposure to visible light, these spiropyran molecules return to their original polarity, the micelle reassembles, and it re-encapsulates about 40% of the cross-linkers it previously released.

Light-responsive micelles are an exciting avenue to pursue in SLA printing because of the potential ability to rapidly release precise amounts of chemicals, at precise locations, and at precise times. Light-responsive micelles open up new possibilities for polymerization techniques by introducing a light-induced mechanism to otherwise spontaneous reactions. For example, Zhang *et al.* (2016) described a one-pot polymerization mechanism in which a mixture of chitosan and L-dopa spontaneously cross-linked upon addition of sodium iodate. If a light-responsive micelle were used to control the addition of sodium iodate, it could cause localized polymerization in the vat of resin, thereby creating a new photopolymerization mechanism using micelles. Besides the prospect of new avenues of light-induced polymerization, micelles improve health and environmental safety performance by mitigating exposure to hazardous cross-linkers, reactive oligomers and monomers, and photoinitiators. However, utilizing light-induced micelles in SLA printing is a new idea and requires extensive research before it can be considered a viable solution. While using micelles in SLA printing may be far from commercially-ready, it remains an exciting avenue to pursue and may change the way we think about SLA printing.

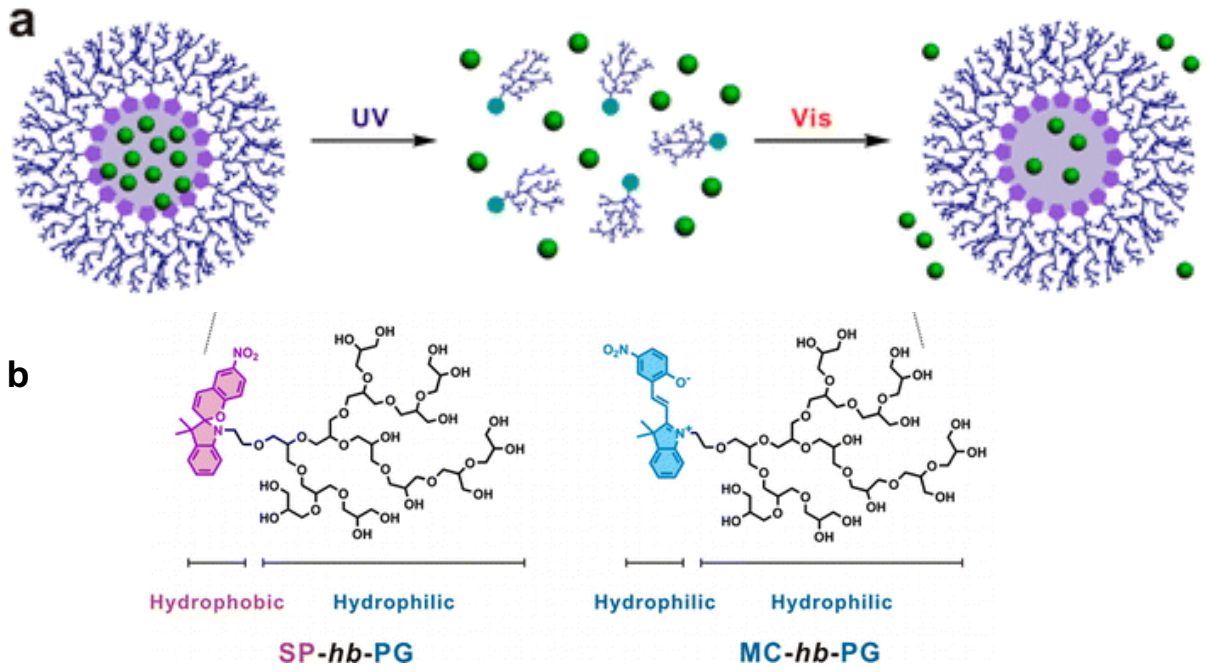

Figure 7. (a) Schematic for the spiropyran hyperbranched polyglycerol micelle upon exposure to UV and visible light. (b) The reversible change in polarity in the spiropyran moiety upon exposure to UV light (Adapted from *Son et al., 2014*).

Health and Environmental Performance

The toxicity of micelles is largely dependent on their design and specific application. In the Son *et al*. study (2014) discussed above, spiropyran initiated hyperbranched polyglycerols were found to be non-toxic to WI-38 and HeLa cell lines in cytotoxicity assays. This is a promising result from one particular micelle technique that could theoretically be applied in the SLA context.

Because of the diversity of options within the field of encapsulation techniques, classifying the toxicity of the micelles with any confidence remains a challenge. Even so, the high degree of control over ingredients and mechanisms allows for health and environmental concerns to be considered and incorporated during the design phase. Certainly, some micelles, such as soaps that have been used for hundreds of years, can be presumed to be fairly benign.

A study that examined the nanotoxicity of micelles affirms the view that micelle toxicity is highly variable. Zhao *et al*. (2013) found that nanotoxicity is correlated with the unique structure of the micelle. Yet, even when examining the same micelle, this study observed different biosafety results in different cell models and found no correlation between animal and *in vitro* tests. These findings underscore the complex nature of micelle toxicity. Any strategy that adopts micelle technology would require extensive analysis across nearly every hazard endpoint prior to development.

Comparison of Alternatives

Technical Performance Summary

A table synthesizing the technical performance of each proposed strategy is found below in Table 10 along with explanations for the comparative performance ranking we assigned to each criterion in Table 11.

As was discussed previously, the functionalized biopolymer strategy is the most technically developed at this point, with reported BSA-based prints meeting all of our technical performance criteria, and with other strong proof-of-concept materials such as functionalized chitosan. It should be noted that this high-ranking performance still relies on acrylate-based cross-linking but that this strategy represents a significant improvement in user exposure to (meth)acrylates, and that a lower weight percent of acrylate co-monomer is used in the proposed formula. In addition, this strategy includes the added value of mechanical tunability via post-print curing and the use of additives.

The lignin-based click chemistry method had acceptable levels of strength, but more insight is needed regarding the curing speed and the accuracy of prints.

For the pH-induced collagen strategy, the biggest strengths were the ability to print parts at a micrometer-scale layer thickness, albeit using an extrusion-based printing method rather than SLA. The tuning of composite formulas to improve mechanical strength requires further testing. More research efforts are also needed to assess print speed.

The spider silk-inspired strategy featured impressive strength and speed, though research is necessary to demonstrate the feasibility of this strategy in a layer-by-layer printing context. As was discussed, this testing should be seriously considered given the impressive strength metrics produced by this material.

Lastly, the micelle strategy features many data gaps. This strategy would require a partner willing to engage in novel research to demonstrate and test the capabilities of encapsulation techniques in an SLA context.

Table 10. Color-coded technical performance comparison table.

Technical Performance Rating (Product Specifications)			
Strategy	Speed	Accuracy	Strength
PR48	1	1	1
Biobased Polymers	1	1	1
Click Chemistry	2	U	1
pH Induced	U	2	2
Spider Silk	2	U	1
Micelles	U	U	U

Legend			
(1) High Performance	(2) Medium Performance	(3) Low Performance	(U) Unknown

Table 11. Rubric for evaluating technical performance rankings.

Red	Yellow	Unknown	Green
- Data is available and well below performance criteria. - No strategy is readily available to reconcile deficiencies. - Significant research is needed in order to reach performance criteria.	- The application does not have performance that matches industry standards, but there are potential, feasible solutions to help reconcile deficiencies. - Data on the particular performance may not have been explicitly reported, but some implicit evidence was provided for high or medium performance.	- Data does not exist at all. - No evidence is available to suggest the performance **would or wouldn't** meet industry standards. - In need of significant research and development in order to close the data gap.	- Has been demonstrated and meets performance criteria.

Health and Environmental Performance Summary

Each proposed strategy has distinct benefits compared to PR48 with regards to health and environmental performance. The bio-based polymers strategy improves on systemic toxicity; pH induced photo-polymerization features lower systemic toxicity, skin and eye irritation, skin and respiratory sensitization, and ecotoxicity; micelles allow for health and environmental concerns to be considered in the design phase; and nearly all of the strategies benefit from using chemicals that can be sustainably sourced. When considering each strategy, we looked across an array of toxicological and environmental endpoints to ensure that we did not substitute one hazard for another. In addition, we considered hazards across the lifecycle of the chemicals involved in the strategies. Although exposure hazards may be reduced for SLA users who handle the prints using biopolymer-based strategies, they remain concerning for workers involved in manufacturing the resins. Our hazard ratings in Table 11 account for the maximum hazard across the chemical lifecycle. Explanations for our rating system are provided in Table 13.

For almost all of our strategies, data gaps persist for some of the most important endpoints, including cancer and reproductive and developmental toxicity (Table 12). Further investigation into these endpoints must be conducted before these strategies can be safely developed or upscaled.

Table 12. Color-coded human health / environmental hazard comparison table.

Health/Environmental Performance Rating					
Strategy	Carcinogenicity, Mutagenicity, Reproductive/ Developmental, Endocrine Disrupting	Systemic Toxicity	Skin, Eye, Respiratory Irritation/ Sensitization	Ecotoxicity	Sustainably Sourced Chemical
PR48	2	2	3	2	3
Biobased Polymers	U	1	3	2	1
Click Chemistry	2	2	3	2	1
pH Induced	U	1	2	1	1
Spider Silk	U	2	3	2	2
Micelles	U	U	U	U	U

Legend			
(1) Low Hazard	(2) Medium Hazard	(3) High Hazard	(U) Unknown

Table 13. Rubric for assigning health and environmental rankings.

Red	Yellow	Unknown	Green
- Authoritative lists, toxicity data, and/or safety data sheets indicate that components of the alternative solution are harmful via one or more of the endpoints listed in the column header and that the hazard is high. - Components were considered high hazard if they were especially toxic or if they were moderately toxic but present in high concentrations (>50%). - Levels of toxicity were determined by GHS classification criteria for irritation, sensitization, systemic toxicity, and ecotoxicity. IARC classifications were used for carcinogenicity (IARC Groups 1 and 2A were considered high hazard).	- Everything not classified under the red, green, or gray categories was categorized as yellow.	- Toxicity data was not available for components of the alternative solution at the stated endpoints.	- Toxicity data indicate that the components of the alternative solution are generally low hazard at the stated endpoints as defined by GHS criteria or other widely-adopted standards.

Overall Performance Summary

To more clearly demonstrate the benefits and trade-offs of our proposed strategies, we compiled the above information into an overall comparison in Table 14. This table summarizes the health, environmental, and technical performance of each of our strategies throughout the resin life cycle. The first two columns (Health Criteria - “Formulation” and “Printing/Use”) represent the human health risks posed during resin formulation and during the printing of objects/use of printed objects. For our first two strategies, we propose functionalizing

biopolymers with reactive functional groups that cross-link during printing. In these strategies, the raw ingredients include toxic substances that present a hazard during the preparation of functionalized biomolecules. However, the formulated resin is comprised of molecules that are not bioavailable because their high molecular weight and low volatility preclude skin penetration and inhalation exposure. Thus, relative to PR48, these strategies remove the risk for users of SLA-printed objects and SLA printers, but still present a risk to workers who prepare SLA resins.

In contrast, the pH-induced polymerization strategy does not contain hazardous components aside from the photo base generator, which should be further explored. The spider silk strategy includes ammonium persulfate in both the formulation and printing stages, which may present a health risk to formulators and users, although it is present at low concentrations and could be replaced by an alternative photoinitiator.

The Technical - “Printing/Use” column indicates an overall technical performance score for each strategy. Whereas PR48 and the acrylate-functionalized biopolymer strategy meet all of our technical performance criteria, several of our strategies show inadequate performance in one or more criteria. We believe the performance of these strategies could be improved with further SLA-focused development of these technologies, and we see potential for each to become a high-performing strategy.

Finally, we assessed the potential environmental impacts of each strategy in the “Waste Disposal” column. A major environmental consideration for SLA printing is the disposal of used resins and the potential for production of hazardous waste. For example, the existing PR48 formula contains ecotoxic components, and the unreacted acrylates are removed from the printed objects in solvent baths, generating hazardous waste. The ingredients in our proposed strategies present lower ecotoxicity than PR48 and do not use post-print solvent baths, thereby reducing or eliminating toxic waste disposal and reducing potential environmental impact.

Table 14. Overall comparison of performance across product lifecycle.

Strategy	Health Criteria		Technical	Environmental
	Formulation	Printing/Use	Printing/Use	Waste Disposal
PR48	3	3	1	3
Biobased Polymers	3	1	1	2
Click Chemistry	3	1	2	2
pH Induced	1	1	2	1
Spider Silk	2	2	2	2
Micelles	U	U	U	U

Legend			
(1) High Performance	(2) Medium Performance	(3) Low Performance	(U) Unknown

Conclusions & Recommendations

As the SLA printing industry continues to grow it is imperative to improve upon current acrylate-based resins like PR48. The five strategies outlined in this report uniquely address our criteria with respect to technical performance and health and safety. The level of development for each of these strategies was determined with respect to the following stages: preliminary research, proof-of-concept, assess areas for improvement, and prototyping (Table 15).

Table 15. Development stages of proposed strategies.

	Preliminary Research	Proof-of-concept	Assess areas for improvement	Prototyping
Biopolymers				Consider post-print curing for enhanced strength
Click chemistry			Test modifications to improve print speed	
pH induced		Assess alternative photo base generators, test print with hydroxyapatite		
Spider silk		Test layer-by-layer printing Consider post-modification, Ru alternatives		
Micelles	Find research partners to develop & demonstrate technology			

The methacrylate-functionalized biopolymers strategy is our most developed and market-ready strategy. A BSA-based resin has already been printed using a commercial SLA printer. The next steps in prototyping this resin include optimizing UV and thermal post-print cure steps to obtain the desired mechanical properties. Additionally, alternatives to the ruthenium-based photoinitiator should be explored in order to avoid potential hazards and costs associated with ruthenium. Another potential health hazard with the current BSA-based formula is the inclusion of acrylate oligomers not bound to BSA. Further testing with lower weight percentages of acrylate oligomer should be conducted to determine whether adequate mechanical properties can be achieved without these components. Furthermore, although functionalized chitosan and BSA represent likely improvements to the PR48 formula with regards to health and environmental impact, there remain significant data gaps on a number of important endpoints including carcinogenicity and reproductive and developmental toxicity. Further development of this strategy should include toxicity testing for these components. These factors should all be considered during further development of biopolymer-based resins.

The use of lignin modified with click chemistry-enabled functional groups has been partially demonstrated but requires significant further assessment with respect to multiple technical performance endpoints. First, the ability to attach both reactive functional groups (i.e.,

maleimide and furan or benzophenone) to lignin must be confirmed. Then, the use of functionalized lignin as the reactive cross-linker must be optimized for speed and accuracy. This optimization process may include varying the density of functional groups attached to the lignin backbone and adjusting the molecular weight of lignin polymers used, among other variables. A potential challenge for this strategy is the need for low viscosity to achieve a high dimensional accuracy, whereas lignin tends to induce a high viscosity in liquids. Due to the multiple endpoints that require further development, several cycles of optimization and prototyping may be necessary to achieve a resin meeting all technical requirements with this strategy.

The pH-induced strategy requires proof-of-concept of our proposed modifications, followed by further assessment of techniques to improve resin performance. Specifically, the use of collagen-ribose-hydroxyapatite composite materials has not been demonstrated in an SLA context, so requires initial verification that these materials will photo-cure with the use of a photo base generator. Following the demonstration of this strategy, we anticipate that additional improvements will be desired, particularly with respect to print speed. Optimization may include varying the relative proportions of each ingredient. In addition, we anticipate the ribose sugar cross-linking of collagen to be a slow step, which may require further modification, for instance via pre-processing at the formulation stage. We also recommend testing alternative photo base generators and minimizing their concentration in the resin formula since these ingredients present the greatest hazard for this strategy.

The strategy using cross-linking of unmodified proteins requires a proof-of-concept as well as an investigation into improving aspects of the photo-cross-linking mechanism and resin to meet technical performance. Concerns remain regarding the ruthenium-based photoinitiator system used in this strategy, and as with the BSA-based resins, alternatives should be considered. The recombinant spider silk proteins were shown to successfully cross-link upon exposure to 465 nm light, however, the viscosity of the resin is unknown, and the resin was cross-linked in a mold as opposed to a layer-by-layer fashion used in SLA printing. Thus, this technique should be tested using a layer-by-layer print in order to determine whether it has adequate dimensional accuracy and curing speed. Additionally, this method may require changes to the light source in SLA printers, since the technique was demonstrated using light at a wavelength of 635 nm.

Lastly, the use of light-responsive micelles in SLA printing is a potential strategy that would require extensive research before it could be implemented. First and foremost, a highly controllable micelle system must be developed to release reactive components for polymerization. The development of novel micelles will likely be the most time-intensive step since the micelle must be able to hold specific reactive molecules while also remaining intact and stable against the external solvent environment. Once such a micelle system is developed, additional research will be necessary to control the amount and rate of chemical release. Lastly, we recommend the development of a re-encapsulation mechanism, as described in the spiropyran hyperbranched polyglycerol example, to mitigate exposure to hazardous resin components. While using micelles in SLA printing will require extensive research prior to commercial use, this strategy remains an exciting avenue to pursue and has the potential to revolutionize SLA printing technology.

As the SLA industry grows, potential harm to health and the environment becomes amplified. This report provides a roadmap for developing safer resins by proposing five strategies that offer distinct advantages relative to acrylate-based resins such as PR48. We hope that these strategies provide industry actors with the foundation to create SLA resins that uphold principles of health, the environment, and sustainability.

References

Allnex. (2019). Safety Data Sheet EBECRYL® 8210 radiation curing resins. Retrieved from: https://www.allnex.com/en/product/8336c301-c795-4725-94b1-09b2777c4a70/ebecryl-8210
Arkema (2014). SAFETY DATA SHEET SR494. Retrieved From: https://www.arkema.com/media/downloads/socialresponsability/safety-summuries/

Autodesk. (n.d.) Autodesk Standard Clear Prototyping Resin (PR48). Retrieved from: https://cdn2.hubspot.net/hubfs/1545937/Autodesk_Standard_Clear_PR48

Beach, E., Kundu, S. (2017). Tools for Green Chemistry. Wiley & Sons. Retrieved from: https://books.google.com/books=acrylates+in+SLA

Buono, P.; Duval, A.; Averous, L.; Habibi, Y. (2017). Thermally healable and remendable lignin-based materials through Diels-Alder click polymerization. Polymer. 133, 78-88.

ChemSafetyPro. (2019). Degradation. Retrieved from: https://www.chemsafetypro.com/Topics/CRA/degradation.html

Cheng, C., Dennis, A., Hill, L., Rainey, C., Rodriguez, B. (2015). Autodesk and Stereolithography 3D Printing: Bio-inspired Resins for Better Human and Environmental Health. Retrieved from: https://bcgctest.files.wordpress.com/2017/04/final-reportautodesk_greenersolutions_2015.pdf

Dams-Kozlowska, H., Majer, A., Tomasiewicz, P., Lozinska, J., Kaplan, D. L., & Mackiewicz, A. (2013). Purification and cytotoxicity of tag-free bioengineered spider silk proteins. Journal of biomedical materials research. Part A, 101(2), 456–464. doi:10.1002/jbm.a.34353

Gil, D. (2018). Enhancing Spider Silk Protein Materials through Continuous Electrospinning and Photo-initiated Cross-linking. Retrieved from: https://digitalcommons.usu.edu/cgi/viewcontent.article

Guaresti, O.; Garcia-Astrain, C.; Palomares, T.; Alonso-Varona, A.; Aceiza, A.; gabilondo, N. (2017). Synthesis and characterization of a biocompatible chitosan-based hydrogel cross-linked via 'click' chemistry for controlled drug release. International Journal of Biological Macromolecules. 102, 1-9.

Herner, A.; Lin, Q. (2016). Photo-Triggered Click Chemistry for Biological Applications. Top Curr Chem (J). 374(1), 1-37.

Holten-Andersen, N.; Harrington, M. J.; Birkedal, H.; Lee, B. P.; (2011). Messersmith, P. B.; Lee, K. Y. C.; Waite, J. H. pH-induced metal-ligand cross-links inspired by mussel yield self-healing polymer networks with near-covalent elastic moduli. PNAS. 108(7), 2651-2655.

Hu, Xiaohong, and Changyou Gao. (2008). Photoinitiating Polymerization to Prepare Biocompatible Chitosan Hydrogels. Journal of Applied Polymer. Science. 110(2), 1059–1067.

International Agency for Research on Cancer. (2012). IARC Monographs: Benzophenone. Retrieved from: https://monographs.iarc.fr/wp-content/uploads/2018/06/mono101-007.pdf

Inzana, J. A.; Olvera, D.; Fuller, S. M.; Kelly, J. P.; Graeve, O. A.; Schwartz, E. M.; Kates, S. L.; Awad, H. A. (2014). 3D Printing of Composite Calcium Phosphate and Collagen Scaffolds for Bone Regeneration. Biomaterials. 35(13), 4026-4034.

Jarosz T, Gebka K, Stolarcyk A. (2019). Recent Advances in Conjugated Graft Copolymers: Approaches and Applications. Molecules. 24(16), 3009.

Kaza A, Rembalsky J, Roma N, Yellapu V, Delong WG, Stawicki SP. (2018). Medical applications of stereolithography: An overview. Int J Acad Med [serial online] ;4:252-65. Retrieved from: http://www.ijam-web.org/text.asp?2018/4/3/252/248331

Kim, S. S.; Lau, C. M.; Lillie, L. M.; Tolman, W. B.; Reineke, T. M.; Ellison, C. J. (2019). Degradable Thermoset Fibers from Carbohydrate-Derived Diols via Thiol-Ene Photopolymerization. Applied Polymer Materials. 1, 2933-2942.

Krishnakumar, G. S.; Gostynska, N.; Compodoni, E.; Dapporto, M.; Montesi, M.; Panseri, S.; Tampieri, A.; Kon, E.; Marcacci, M.; Sprio, S.; Sandri, M. (2017). Ribose mediate cross-linking of collagen-hydroxapatite hybrid scaffolds for bone tissue regeneration using biomimetic strategies. Materials Science and Engineering: C. 77, 594-605.

Lee, A.; Hudson, A. R.; Shiwarski, D. J.; Tashman, J. W.; Hinton, T. J.; Yerneni, S.; Bliley, J. M.; Campbell, P. G., Feinberg, A. W. (2019). 3D bioprinting of collagen to rebuild components of the human heart. Science. 365(6452), 482-487.

Mason, B. N.; Starchenko, A.; Williams, R. M.; Bonassar, L. J.; Reinhart-King, C. A. (2013). Tuning three-dimensional collagen matrix stiffness independently of collagen concentration modulates endothelial cell behavior. Acta Biomaterialia. 9(1), 4635-4644.

Meador, M. A. B.; Meador, M. A.; Williams, L. L.; Scheiman, D. A. (1996). Diels-Alder Trapping of Photochemically Generated Dienes with a Bismaleimide: A New Approach to Polyimide Synthesis. Macromolecules. 29(27), 8983-8986.

Meat and Livestock Australia. Manufacture of Bovine Serum Albumin. (2001). https://meatupdate.csiro.au/infosheets/ManufactureofBovineSerumAlbumin.pdf

Melchels, F. P. W., Feijen, J., Grijpma, D. (2010). A review on stereolithography and its applications in biomedical engineering. Retrieved from: https://www.sciencedirect.com/science/article/

Noff, M.; Pitaru, S. (2003). Cross-linked collagen matrices and methods for their preparation. European Patent Office: EP1280545A4.

Norweigan Scientific Committee for Food Safety. (2016). Risk assessment of "other substances" – Collagen from fish skin. VKM. Retrieved from: https://vkm.no/download/18.pdf

Pourhaghgouy, M.; Zamanian, A.; Shahrezaee, M.; Masouleh, M. P. (2016). Physicochemical Properties and Bioactivity of Freeze-Cast Chitosan Nanocomposite Scaffolds Reinforced with Bioactive Glass. Materials Science and Engineering: C. 58, 180–186.

Rahn. (2018). Safety Data Sheet: Genomer 1122.

Radl, S. V.; Schipfer, C.; Kaiser, S.; Moser, A.; Kaynak, B.; Kern, W.; Schlogl, S. (2017). Photo-responsive thiol-ene networks for the design of switchable polymer patterns. Polymer Chemistry 8, 1562-1572.

Sahu, A. K., Dash, D. K., Mishra, K., Mishra, S. P., Yadav, R., Kashyap, P. (2017). Properties and Applications of Ruthenium. Intech Open. DOI: 10.5772/intechopen.76393

Saikia C., Gogoi P., Maji TK. (2015). Chitosan: A Promising Biopolymer in Drug Delivery Applications. J Mol Genet Med 4(006).

Schmidleithner, C., Kalaskar D. M. (2018). Stereolithography. Intech Open. DOI: 10.5772/intechopen.78147

Schweigert, N.; Zehnder, A. J. B.; Eggen, R. I. L. (2001). Chemical properties of catechols and their molecular modes of toxic action in cells, from microorganisms to mammals. Environmental Microbiology. 3(2), 81-91.

Sharma, R. (2013). The 3D Printing Revolution You Have Not Heard About. Forbes. Retrieved from: https://www.forbes.com/sites/rakeshsharma/

Sigma-Aldrich. (2014). Safety Data Sheet: Ammonium Persulfate. Retrieved from: https://www.sigmaaldrich.com/MSDS/ammoniumpersulfate

Sigma-Aldrich. (2019). Safety Data Sheet:Tris(2,2′-bipyridyl)dichlororuthenium(II)hexahydrate. Retrieved from: https://www.sigmaaldrich.com/MSDS/ruthenium

Smith, P. T.; Narupai, B.; Tsui, J. H.; Millik, S. C.; Shafranek, R. T.; Kim, D. H.; Nelson, A. (2019). Additive Manufacturing of Bovine Serum Albumin-Based Hydrogels and Bioplastics, ChemRxiv [Preprint], 9758876.

Son, S., Shin, E., Kim, B. (2014). Light-Responsive Micelles of Spiropyran Initiated Hyperbranched Polyglycerol for Smart Drug Delivery. Biomacromolecules 2014, 15, 2, 628-634. https://doi.org/10.1021/bm401670t

ToxNet. (2015). Benzophenone. Retrieved from: https://toxnet.nlm.nih.gov/cgi-bin/sis/search/a?dbs+hsdb:@term+@DOCNO+6809

ToxNet. (2015). Maleic Acid. Retrieved from: https://toxnet.nlm.nih.gov/cgi-bin/sis/search/a?dbs+hsdb:@term+@DOCNO+666

ToxNet. (2000). Hydroxyapatite. Retrieved from: https://toxnet.nlm.nih.gov/cgi-bin/sis/search/a?dbs+hsdb:@term+@DOCNO+5804

Tyson, D. S.; Ilhan, F.; Meador, M. A. B.; Smith, D. D.; Sheriman, D. A.; Meador, M. A. (2005). Diels-Alder Trapping of Photochemically Generated o-Quinodimethane Intermediates: An Alternative Route to Photocured Polymer Film Development. Macromolecules. 38(9), 3638-3646.

UK Marine Special Areas of Conservation. (n.d.). Standard criteria for toxicity profiles. Retrieved from: http://www.ukmarinesac.org.uk/activities/water-quality/wq3_1_2.htm

United Nations. (2011). Globally Harmonized System of Classification and Labelling of Chemicals (GHS). 4th ed. Retrieved from: https://www.unece.org/fileadmin/DAM/trans/

Varotsis, A. B. (2019). Introduction to SLA 3D Printing. Retrieved from: https://www.3dhubs.com/knowledge-base/introduction-sla-3d-printing/#work

Wahl, D. A.; Czernuszka, J. T. (2006). Collagen-Hydroxyapatite Composites for Hard Tissue Repair. European Cells and Materials. 11, 43-56.

Waite, J. H. (2017). Mussel adhesion - essential footwork. Journal of Experimental Biology. 220, 517-530.

Williams, C. G.; Malik, A. N.; Kim, T. K.; Manson, P. N.; Elisseeff, J. H. (2005). Variable cytocompatibility of six cell lines with photoinitiators used for polymerizing hydrogels and cell encapsulation. Biomaterials. 26(11), 1211-8.

Winkler, M.; Mueller, J. O.; Oehlenschlaeger, K. K.; de Espinosa, L. M.; Meier, M. A. R.; Barner-Kowollik, C. (2012). Highly Orthogonal Functionalization of ADMET Polymers via Photo-Induced Diels-Alder Reactions. 45(12), 5012-5019.

Zhang, X.; Hassanzadeh, P.; Miyake, T.; Jin, J.; Roland, M. (2016). Squid beak inspired water processable chitosan composites with tunable mechanical properties. Journal of Materials Chemistry B. 4, 2273-2279.

Zhao, B., Wang, X., Wang, X. (2013). Nanotoxicity comparison of four amphiphilic polymeric micelles with similar hydrophilic or hydrophobic structure. Part Fibre Toxicol 10, 47 doi:10.1186/1743-8977-10-47